Journal of Radioanalytical and Nuclear Chemistry (2018) 318:149–155
https://doi.org/10.1007/s10967-018-6113-9

Primary standardization of the massic activity of a ^{233}Pa solution

R. Fitzgerald[1] · L. Pibida[1]

Received: 10 April 2018 / Published online: 23 August 2018

Abstract
Protactinium-233 (^{233}Pa) is used as a tracer for radiochemical analysis and is of particular interest as an isotope dilution mass spectrometry (IDMS) spike for ^{231}Pa/^{235}U radio-chronometry. To this end, we present massic activity determinations by two methods for a ^{233}Pa solution, which was prepared at Lawrence Livermore National Laboratory (LLNL) and is being characterized at multiple labs as part of a ^{231}Pa reference material production project. One activity determination method was 4πβ-γ anti-coincidence counting in a multi-dimensional extrapolation model, with Monte Carlo corrections. An independent massic activity determination was completed by γ-ray spectrometry using 5 high purity germanium (HPGe) detectors using 5 γ-ray lines. The anti-coincidence and γ-ray spectrometry results agree and have combined standard uncertainties of about 0.33% and 1.0% respectively. In addition, the two methods were combined to derive γ-ray emission probabilities from ^{233}Pa decay.

Keywords Protactinium-233 · Pa-233 · ^{233}Pa · Activity · IDMS spike · Gamma-ray emission probability

Introduction

Protactinium-233 (^{233}Pa) is an important tracer for radiochemical analysis of ^{231}Pa [1–3]. Whereas ^{231}Pa undergoes alpha decay without significant γ-ray emission, ^{233}Pa decays by β-particle emission accompanied by numerous γ-rays (Fig. 1); as such the ^{231}Pa γ-ray signal can be used for monitoring Pa separations.

In the field of nuclear forensics, there is an outstanding challenge for producing well-characterized ^{233}Pa solutions for use as a spike in Isotope Dilution Mass Spectrometry (IDMS) analysis of ^{231}Pa for ^{231}Pa/^{235}U dating [4, 5]. The present work is motivated by a project led by Lawrence Livermore National Laboratory (LLNL) to produce a reference material characterized for amount of ^{231}Pa. This reference material will allow for traceable calibrations of the necessary short-lived ^{233}Pa spikes (half-life: 26.98 ± 0.02 days [6, 7]). That project requires a ^{233}Pa spike with well characterized concentration (mol/g) for reverse-IDMS measurements. One method for obtaining that concentration is to measure the ^{233}Pa massic activity (Bq/g) of the spike solution and then use the half-life to convert to concentration. To that end, LLNL sent aliquots of their spike solution to multiple radionuclide metrology laboratories for assay. Here, we report the results from the National Institute of Standards and Technology (NIST).

This project presented an opportunity to measure the massic activity by live-timed 4πβ-γ anticoincidence counting (LTAC) of a very pure ^{233}Pa solution. Previous standardizations have relied on the equilibrium conditions of ^{233}Pa with its parent ^{237}Np, taking advantage of the relative ease of measuring absolute alpha decay of ^{237}Np rather than beta decay of ^{233}Pa [8–17]. In some of those works, both nuclides were measured in equilibrium using 4πβ-γ coincidence [15, 16]. The γ-ray emission probabilities (P_γ) for ^{233}Pa decay have been evaluated [7, 14, 18]. The P_γ for the 312 keV transition as measured by [17] differs significantly from the evaluated value. A subsequent study [10] agrees with the evaluated value. The P_γ in question has implications for the ^{237}Np and ^{232}Th neutron capture cross sections. The present work provides an independent measurement of the 312-keV P_γ.

✉ R. Fitzgerald
ryan.fitzgerald@nist.gov

[1] NIST, 100 Bureau Drive, Gaithersburg, MD 20899, USA

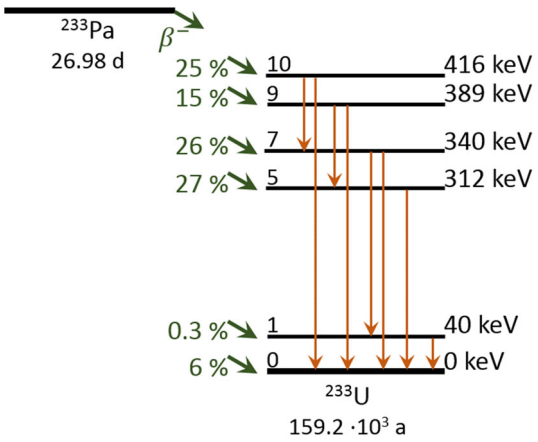

Fig. 1 Simplified ^{233}Pa decay scheme. Adapted from DDEP [6, 7]

Experimental

Source preparation

The final purification of the ^{233}Pa solution occurred at LLNL on 27 June 2017 at 15:50 PDT, which serves as the reference time for the activity measurements reported here. The solution consisted of 2 mol L^{-1} HNO_3 + 0.1 mol L^{-1} HF. The activity ratio of ^{237}Np to ^{233}Pa at separation was $<1 \cdot 10^{-8}$ [Williams, R.W.; personal communication 2017]. Approximately 5.3 g of the ^{233}Pa solution was shipped to NIST in a Teflon vial.

In July 2017, the LLNL vial was opened at NIST. Approximately 0.04 g to 0.16 g was transferred gravimetrically into each of 8 liquid scintillation (LS) vials containing 4 mL of either "Ultima Gold"[1] (2 vials) or "Ultima Gold AB" scintillants (Perkin Elmer, Waltham, MA, USA). Additional 2 mol L^{-1} HNO_3 carrier was added to bring the aqueous content of the LS sources up to 2% for Ultima Gold and 6% for Ultima Gold AB. The ^{233}Pa solution was diluted with carrier by a factor of 1.2960 ± 0.0006 for gravimetrically filling a standard 5 mL NIST ampoule [19] for which our high purity germanium (HPGe) detectors are calibrated. All of the gravimetric transfers were done by measuring by difference the masses of solution dispensed from an aspirating polyethylene pipette ("pycnometer") using a 6-digit microbalance.

4πβ-γ anticoincidence measurements

The 4πβ-γ anticoincidence (LTAC) method was used to determine the massic activity of the ^{233}Pa solution. The NIST LTAC system and Monte Carlo analysis method have been described previously [20, 21]. In brief, the 4πβ detector consists of a liquid scintillation (LS) source coupled to a single photomultiplier tube. The γ-ray (and X-ray) detector is a NaI(Tl) well detector. A digital data acquisition system is used to record the pulse heights and time stamps from both detectors. The data are processed offline by the multiple channel anticoincidence method with shared, controllable extending dead time [22]. The LS efficiency is varied by changing the lower-level discriminator for the LS amplitude in the software.

Up to 3 NaI(Tl) gates were used in anti-coincidence mode to monitor the LS inefficiency for three different subsets of decays. The output of the data processing was the LS rate (N_{LS}), and the NaI(Tl) anticoincident-to-total ratios (Y_i) for each of the 3 gates. A linear combination of the Y_i is adopted as the effective LS inefficiency,

$$Y_{\text{eff}} = \sum a_i Y_{\text{i}}, \tag{1}$$

where the a_i are weighting factors. Either a linear or quadratic least-squares fit of the LS rate (N_{LS}) vs. Y_{eff} is carried out and extrapolated to $Y_{\text{eff}} = 0$, to obtain the nominal source decay rate (N_0). The linear fit equation with free parameters N_0, k, and the a_i is,

$$N_{LS} = N_0(1 - kY_{\text{eff}}) \tag{2}$$

Due to the complex decay scheme, N_0 from the fit can differ from the true activity. To correct for this, a Monte Carlo simulation, using Geant4 library [23], of the entire experiment was performed with identical extrapolations as for the data. A correction factor, F, was derived by the ratio of N_0 to the "true" activity input to the Monte Carlo.

The final massic activity (A) was determined for each source from N_0, F, and mass, m of the ^{233}Pa solution in the source.

$$A_m = \frac{FN_0}{m} \tag{3}$$

The free parameter in the Monte Carlo simulation is the scintillation efficiency, which was set to 4500 UV photons per MeV of electron energy, which matched the experimental LS spectrum (Fig. 2). The three NaI(Tl) gates were set to be sensitive to various decay pathways (Table 1), such that the LS efficiency for each path could be extrapolated to 100% ($Y_i = 0$). Since ^{233}Pa does have a significant β branch to the ^{233}U ground state (β_0), without emission of a photon, the LS efficiency of that branch is not monitored by any of the gates. However, since all the β spectra are of similar shape (same nucleus, all first-forbidden), one can use a linear combination of Y_i's from other transitions to represent the inefficiency for detecting β_0 [22]. However, given the complicated decay scheme, including numerous conversion electrons, achieving a linear extrapolation using the three Y_i values is not necessarily

[1] Any mention of commercial products is for information only; it does not imply recommendation or endorsement by NIST.

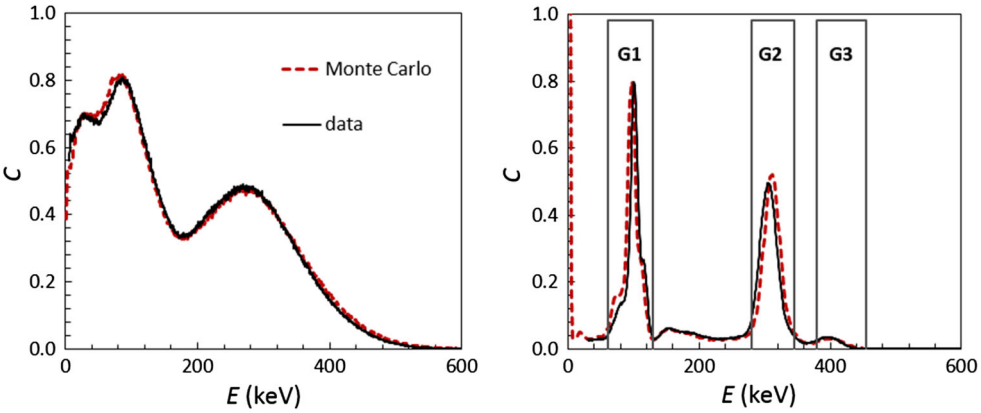

Fig. 2 Measured (solid black lines) and simulated (dashed red lines) spectra from LS (left) and NaI(Tl) (right) detectors, where C is counts with arbitrary scaling and E is approximate energy, proportional to pulse height. In the LS spectrum, the three peaks correspond to conversion electrons. In the NaI(Tl) spectrum, the three gates used for LTAC are shown

Table 1 Energy gates in the LTAC NaI(Tl) detector

Gate	E (keV)	Photons	Correlated LS events
1	60–130	$\gamma_{10,7}$	$\beta_{10} \rightarrow \gamma_{7,0}$
		$\gamma_{9,5}$	$\beta_9 \rightarrow \gamma_{5,0}$
		X_K	$\beta_{i\geq 5} \rightarrow CE_{5,0}$
2	280–345	$\gamma_{7,0}$	β_7; $\beta_{10} \rightarrow CE_{10,7}$
		$\gamma_{5,0}$	β_5;$\beta_7 \rightarrow CE_{7,5}$
		$\gamma_{7,1}$	$\beta_7 \rightarrow CE_{1,0}$
3	380–455	$\gamma_{10,0}$	β_{10}
		$\gamma_{9,0}$	β_9

For each gate, we list the photon energy range encompassed by the gate, the major γ-ray and X-ray photons detected in the gate, and correlated LS events, whose efficiency is monitored by the coincident photon events. Subscripts correspond to energy levels shown in Fig. 1

possible. Therefore, the Monte Carlo correction, F, was employed throughout.

HPGe detector measurements

Gamma-ray spectrometry measurements were carried out to determine the γ-ray emitting impurities in the source and the source activity. Five different HPGe detectors (both n-type and p-type detectors) with well-characterized efficiency curves [24] were used to determine the source activity. A total of ten measurements were performed for the standard 5 mL NIST ampoule using seven different source measurement geometries. For these different measurement geometries, the sources were placed above and on the side of the HPGe detectors at several source-to-detector distances varying between 20 and 50 cm. For each measurement, the live time was 1 day. The activity was calculated based on the 300.129 keV, 311.904 keV, 340.476 keV, 398.492 keV and 415.764 keV γ-ray peaks and the 2010 DDEP (Decay Data Evaluation Project) evaluated emission probabilities (P_γ's) and half-life [6, 7]. The full-energy-peak efficiency values for the HPGe detectors were previously determined using standard 5 mL NIST ampoules containing calibrated solutions of radionuclides that cover an energy range from 35 to 1.8 MeV and which were placed at the same source-to-detector distances as those used in the present measurements. The efficiency curves were fitted using two different methods (sixth degree polynomial and dual polynomial fit (spline function) with a cross-over point at around 200 keV) in order to assess possible variability in the calculated values for the different γ-ray energies for ^{233}Pa.

Results

4πβ-γ anticoincidence measurements

Each of the 8 LS sources was measured either 2 or 3 times between 7 July 2017 and 28 July 2017 (Fig. 3). No systematic difference was seen between the results for the two LS cocktails, and the source-to-source standard deviation was 0.17%. There was no statistically-significant trend in activity measurement versus time for a given source, averaged over all sources. However, for the four sources that were measured over a longer (5 day) period, three of them showed a decreasing trend of intercept value over time. To conservatively account for any LS cocktail instability, the average decrease in intercept value for those 4 sources was included as an uncertainty component in the massic activity determination.

To check for long-lived impurities, one source was measured again on 4 December 2017, after the ^{233}Pa had decayed by 6 half-lives. The measured activity differed from the mean of the earlier measurements by $(-0.5 \pm 1.4)\%$.[2] This uncertainty would correspond to a limit on long-lived α- or β-emitting impurities of about

[2] All uncertainties reported here are "combined standard uncertainties" [25, 26].

0.04% at the midpoint of the July measurements (2017-07-20 07:00 EST).

Various efficiency extrapolation functions were used to test the sensitivity of the extrapolation intercept to the functional form (linear or quadratic) and number of γ-ray gates (up to 3) included. Example efficiency extrapolations and fit residuals are shown in Fig. 4. The various fits are summarized in Table 2 and the relative results are shown in Fig. 5.

The final value for the LTAC ^{233}Pa massic activity determination was taken as the mean of methods 1, 2, and 3 in Table 2. Those three values were chosen since they included the highest-efficiency LS data, therefore had the shortest extrapolation in Y_{eff}. However, the standard deviation of all 6 values were used in the uncertainty analysis. The final LTAC ^{233}Pa massic activity at the reference time of 27 June 2017 15:50 PDT was $2.361 \cdot 10^4$ Bq g^{-1} with a combined standard uncertainty of 0.33%. The uncertainty analysis is summarized in Table 3.

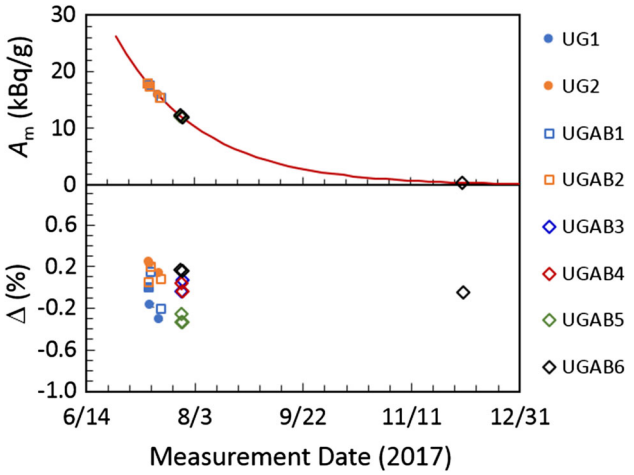

Fig. 3 Decay-corrected LTAC measurement results for 8 LS sources (named in caption). Top: massic activity, A_m. Bottom: decay-corrected A_m plotted as a percent difference (Δ) from the average (excluding the final measurement, used only as an impurity check). Results from linear efficiency extrapolations (Function 1 in Table 2) are shown

Table 2 Summary of extrapolation functions used to analyze the LTAC data

Function	Energy range (keV)	Order	Free parameters
1	14–50	Linear	N_0, k
2	14–50	Linear	a_1, a_2, a_3, N_0, k
3	14–50	Quadratic	N_0, k
4	30–100	Linear	N_0, k
5	30–100	Linear	a_1, a_2, a_3, N_0, k
6	30–100	Quadratic	N_0, k

In cases where the a_i were not free, they were fixed by the best fit to the Monte Carlo simulation results

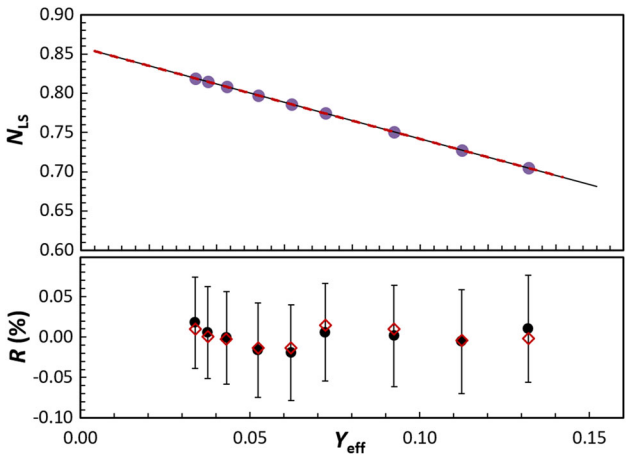

Fig. 4 Example efficiency extrapolation from source UGAB1. Linear (solid black line) and quadratic (dashed red line) are indistinguishable by eye. Residuals for linear (black circles) and quadratic (red diamonds) are shown

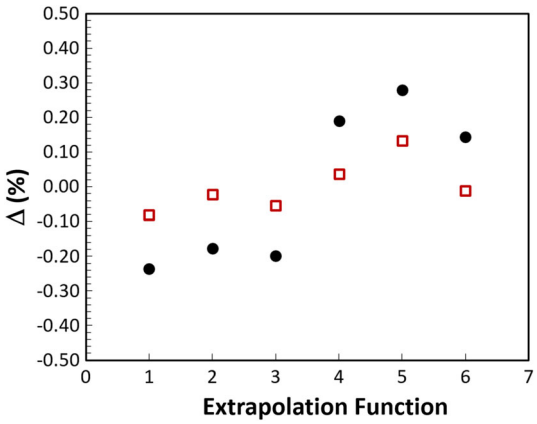

Fig. 5 Percent difference (triangle) from the average result for 6 different extrapolation functions, without (filled cicle) and with (rectangle) Monte Carlo correction factor (F). The corrected values show less model-dependence

HPGe detector impurity measurements

No γ-ray emitting impurities were observed in the source. The estimated limits of detection for the photon-emitting impurities as of August 1, 2017 were: 90 γ s^{-1} for energies between 15 and 35 keV, 20 γ s^{-1} for energies between 40 and 55 keV, 30 γ s^{-1} for energies between 60 and 180 keV, 18 γ s^{-1} for energies between 185 and 280 keV, 40 γ s^{-1} for energies between 258 and 330 keV, 14 γ s^{-1} for energies between 340 and 430 keV, and 4.8 γ s^{-1} for energies between 440 and 2000 keV.

Table 3 Uncertainty evaluation [25, 26] for the LTAC determination of the ^{233}Pa massic activity

Uncertainty component	u_i (%)	Evaluation
Source stability: Average deviation between measured activity for the same source measured 5 days apart, averaged over 4 sources	0.15	A
Source-to-source variability: Standard deviation of the distribution (N = 5) for the extrapolation intercepts of 5 sources. The value for each source was an average of 2 or 3 measurements	0.17	A
Least-squares fit: Uncertainty on extrapolation value due to the fit	0.07	A
Extrapolation range and function: Standard deviation of the distribution (N = 6) for 6 fits spanning 2 LS efficiency ranges, each with its own Y_{eff} weighting. For each range, three fits were carried out: Linear Y_{eff}, Linear 3-gate, Quadratic Y_{eff}. Results were then corrected for bias using Geant4	0.06	A
Geant4 model uncertainty: Uncertainty on the corrections (− 0.09% to 0.22%) using Geant4 model due to nuclear data and matching of model to data	0.17	B
Background: Standard deviation in mean intercept from using various background measurements (7 background measurements made)	0.06	A
Gravimetric links: Estimated uncertainty in the mass of ^{233}Pa solution added to the LS hemispheres based on previous tests	0.05	B
Live-time: Estimated uncertainty in the live time of the counting system, based on limits of previous systematic tests	0.10	B
Half-life: Uncertainty due to DDEP half-life (26.98 ± 0.02) days	0.002	B
Impurities: None seen. From limit on LTAC and HPGe analyses	0.03	B
Combined standard uncertainty: $\boldsymbol{u_c}$ (%)	**0.33**	

Final line reports combined standard uncertainty in bold

Table 4 Uncertainty analysis for the ^{233}Pa massic activity determined by HPGe γ-ray spectrometry

Uncertainty component	u_i (%)	Evaluation
Peak fitting and counting statistics: Standard deviation of the mean value of the peak areas	0.11	A
Gamma-ray emission probabilities: Standard deviation of the mean value of $P_\gamma(E)$	0.73	B
Efficiency: HPGe detector full-energy peak efficiency fit based on measured efficiency curve	0.57	B
Decay correction during measurement: Uncertainty due to the application of a decay correction during the measurement time	0.0005	B
Decay factor: Uncertainty due to the application of a decay factor correction for the source activity from the reference time to the measurement time	0.04	B
Combined standard uncertainty: u_c (%)	**0.93**	

Final line reports combined standard uncertainty in bold

HPGe detector activity determination

The peak areas used to determine the ^{233}Pa activity were obtained using Genie 2000 (Canberra Industries, Inc., Meriden, CT, USA) (using interactive peak fit without the fit singlet option). Due to the low counting rates, no pile-up corrections were necessary. Decay corrections during the measurement time and to the reference time were performed for all measurements. The dilution mass of solution in the HPGe ampoule and dilution factor were used to calculate a massic activity of the NIST-1 solution. The measured massic activity of ^{233}Pa at the reference time was $2.611 \cdot 10^4$ Bq g^{-1} with a combined standard uncertainty of 0.93%. The uncertainty evaluation is summarized in Table 4.

HPGe detector γ-ray emission probability (P_γ) determination

The HPGe measurements of the ^{233}Pa source and the LTAC massic activity determination were used to determine the emission probability of five of the main γ-ray lines. For the determination of the P_γ values, the same corrections as for the HPGe activity determination were applied. The activity of the source used for the HPGe measurements was (59.420 ± 0. 196) kBq at the reference time of 20 July 2017, 7:00 AM EST. The P_γ values determined in this work are listed in Table 5 together with the most-recent values from DDEP [6, 7]. The result for the 312 keV P_γ is shown in Fig. 6, along with recent experimental and evaluation results. The present work is in good agreement with recent evaluations, though disagrees with the anomalously-high P_γ from [17].

Table 5 Measured P_γ values for five main γ-ray lines of ^{233}Pa

Energy (keV)	P_γ (this work)	P_γ (DDEP 2010 [6, 7])
300.129	0.0654 ± 0.0006	0.0660 ± 0.0021
311.904	0.3799 ± 0.0033	0.383 ± 0.005
340.476	0.0444 ± 0.0004	0.0447 ± 0.0003
398.492	0.01405 ± 0.00013	0.01408 ± 0.00014
415.764	0.01729 ± 0.00016	0.01747 ± 0.00007

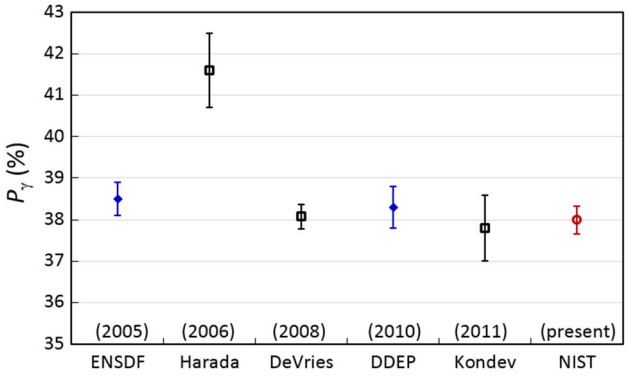

Fig. 6 Recent P_γ results for the 312 keV γ-ray in ^{233}Pa decay. Blue diamonds are evaluations, open squares are previous experimental results and the red open circle is the present work. ENDSF refers to [18] and DDEP to [6, 7]

Discussion

The LTAC determination of ^{233}Pa massic activity using multiple γ-ray gates proved robust against a variety of extrapolation functions. By implementing Monte Carlo correction factors, the variance in extrapolation intercepts among extrapolation functions and efficiency domains was reduced significantly. Furthermore, the lack of radionuclidic impurities detected by both HPGe γ-ray analysis and the consistent LTAC ^{233}Pa activity results over 6 half-lives, indicate that the ^{233}Pa solution is quite pure, making it an excellent reference material.

By combining the $4\pi\beta$-γ anticoincidence result with the evaluated half-life of ^{233}Pa (26.98 ± 0.02) d, and Avogadro's number, we obtain a concentration of the measured ^{233}Pa atom mole concentration at the reference date of $1.471 \cdot 10^{-10}$ mol/kg with a combined standard uncertainty of 0.34%. This can now be used as a reference for isotope dilution mass spectrometry of ^{231}Pa, which was carried out using the solution shortly after separation.

The HPGe γ-ray measurement result for the massic activity of ^{231}Pa agrees with the LTAC value, differing by $(-0.8 \pm 1.1)\%$, where the uncertainty is the combined standard uncertainty on the difference, ignoring small correlations due to half-life. This excellent agreement confirms the LTAC activity value and is also an indication that the uncertainty on the γ-ray emission probabilities used in the HPGe analysis were reasonable. Conversely, by combining LTAC and HPGe measurements, our derived values for the P_γ values are in good agreement with published values. Our value for the strong 312 keV γ-ray agrees with, and has a smaller uncertainty than, the evaluated value. In essence, that result validates our direct measurement of ^{233}Pa by LTAC, compared to earlier indirect values based on ^{237}Np parent measurements and equilibrium assumptions.

Acknowledgements The authors wish to acknowledge Ross Williams and his colleagues at LLNL who provided the ^{233}Pa solution along with leading the larger ^{231}Pa reference material project and our NIST colleague Richard Essex who coordinated the ^{233}Pa and ^{231}Pa measurements at NIST. This work was supported in part by the Department of Homeland Security.

References

1. La Rosa J, Outola I, Crawford E, Nour S, Kurosaki H, Inn K (2008) Radiochemical measurement of ^{237}Np in a solution of mixed radionuclides: experiences in chemical separation and alpha-spectrometry. J Rad Nucl Chem 277(1):11–18. https://doi.org/10.1007/s10967-008-0702-y
2. Sill CW (1978) Radiochemical determination of protactinium-231 in environmental and biological materials. Anal Chem 50(11):1559–1571
3. Morgenstern A, Apostolidis C, Mayer K (2002) Age determination of highly enriched uranium: separation and analysis of ^{231}Pa. Anal Chem 74:5513–5516
4. Eppich GR, Williams RW, Gaffney AM, Schorzman KC (2013) ^{235}U–^{231}Pa age dating of uranium materials for nuclear forensic investigations. J Anal At Spectrom 28(5):666. https://doi.org/10.1039/c3ja50041a
5. Kristo MJ, Williams R, Gaffney AM, Kayzar-Boggs TM, Schorzman KC, Lagerkvist P, Vesterlund A, Ramebäck H, Nelwamondo AN, Kotze D, Song K, Lim SH, Han S-H, Lee C-G, Okubo A, Maloubier D, Cardona D, Samuleev P, Dimayuga I, Varga Z, Wallenius M, Mayer K, Loi E, Keegan E, Harrison J, Thiruvoth S, Stanley FE, Spencer KJ, Tandon L (2018) The application of radiochronometry during the 4th collaborative materials exercise of the nuclear forensics international technical working group (ITWG). J Rad Nucl Chem 315(2):425–434. https://doi.org/10.1007/s10967-017-5680-5
6. Bé M-M, Chisté V, Dulieu C, Mougeot X, Browne E, Chechev V, Kuzmenko N, Kondev F, Luca A, Galán M, Nichols AL, Arinc A, Huang X (2010) Table of radionuclides. BIPM Monographie, vol 5. Sévres
7. Chechev VP, Kuzmenko KN (2010) DDEP Evaluation of Pa-233. Table of Radionuclides
8. Luca A, Etcheverry M, Morel J (2000) Emission probabilities of the main g-rays of ^{237}Np in equilibrium with ^{233}Pa. Appl Rad Isot 52:481–486
9. DeVries D, Griffin H (2008) X- and gamma-ray emissions observed in the decay of ^{237}Np and ^{233}Pa. Appl Radiat Isot 66(5):668–675. https://doi.org/10.1016/j.apradiso.2007.07.019
10. Kondev FG, Ahmad I, Greene JP, Nichols AL, Kellett MA (2011) Measurements of absolute gamma-ray emission probabilities in

the decay of ^{233}Pa. Nucl Instrum Methods Phys Res Sect A 652(1):654–656. https://doi.org/10.1016/j.nima.2011.01.147
11. Schötzig U, Schönfeld E, Janszen H Standardisation and photon emission probabilities in the decay of ^{237}Np/^{233}Pa. Appl Rad Isot 52:883-889
12. Shchukin G, Iakovlev K, Morel J (2004) Analysis of the ^{237}Np-^{233}Pa photon spectrum using the full response function method. Appl Radiat Isot 60(2–4):239–246. https://doi.org/10.1016/j.apradiso.2003.11.024
13. Vaninbroukx R, Bortels G, Denecke B (1984) Determination of photon-emission probabilities in the decay of ^{237}Np and its daughter ^{233}Pa. Int J Appl Radiat Isot 9:905–906. https://doi.org/10.1016/0020-708X(84)90029-2
14. Xiaolong H, Ping L, Baosong W (2005) Evaluation of ^{233}Pa decay data. Appl Radiat Isot 62(5):797–804. https://doi.org/10.1016/j.apradiso.2004.11.005
15. Woods MJ, Woods DH, Woods SA, Husband LJ, Jerome SM, Michotte C, Ratel G, Crespo M, Garcia-Torano E, Rodriguez L, Luca A, Denecke B, Sibbens G, Morel J, Etcheverry M, Santry D, Janssen H, Schönfeld E, Schötzig U (2002) Standardization and decay data of ^{237}Np. Appl Rad Isot 56:415–420. https://doi.org/10.1016/S0969-8043(01)00224-X
16. Woods SA, Woods DH, de Lavison P, Jerome SM, Makepeace JL, Woods MJ, Husband LJ, Lineham S (2000) Standardisation and measurement of the decay scheme data of ^{237}Np. Appl Rad Isot 52:475–479. https://doi.org/10.1016/S0969-8043(99)00197-9
17. Harada H, Nakamura S, Ohta M, Fujii T, Yamana H (2006) Emission probabilities of gamma rays from the decay of ^{233}Pa and ^{238}Np, and the thermal neutron capture cross section of ^{237}Np. J Nucl Sci Technol 43(11):1289–1297. https://doi.org/10.1080/18811248.2006.9711223
18. Singh B, Tuli JK (2005) Nuclear data sheets for A = 233. Nucl Data Sheets 109
19. NIST Ampoule Specifications and Opening Procedure. NIST PML Radiation Physics Division. https://www.nist.gov/pml/radiation-physics/ampoule-specifications-and-opening-procedure. 2018
20. Fitzgerald R (2016) Monte Carlo based approach to the LS–NaI 4πβ-γ anticoincidence extrapolation and uncertainty. Appl Radiat Isot 109:308–313. https://doi.org/10.1016/j.apradiso.2015.11.107
21. Lucas LL (1998) Calibration of the massic activity of a solution of ^{99}Tc. Appl Radiat Isot 49(9–11):1061–1064
22. Baerg AP (1981) Multiple channel 4pb-g anti-coincidence counting. Nucl Instrum Methods 190:345–349
23. Agostinelli S, Allison J, Amako K, Apostolakis J, Araujo H, Arce P, Asai M, Axen D, Banerjee S, Barrand G, Behner F, Bellagamba L, Boudreau J, Broglia L, Brunengo A, Burkhardt H, Chauvie S, Chuma J, Chytracek R, Cooperman G, Cosmo G, Degtyarenko P, Dell'Acqua A, Depaola G, Dietrich D, Enami R, Feliciello A, Ferguson C, Fesefeldt H, Folger G, Foppiano F, Forti A, Garelli S, Giani S, Giannitrapani R, Gibin D, Gómez Cadenas JJ, González I, Gracia Abril G, Greeniaus G, Greiner W, Grichine V, Grossheim A, Guatelli S, Gumplinger P, Hamatsu R, Hashimoto K, Hasui H, Heikkinen A, Howard A, Ivanchenko V, Johnson A, Jones FW, Kallenbach J, Kanaya N, Kawabata M, Kawabata Y, Kawaguti M, Kelner S, Kent P, Kimura A, Kodama T, Kokoulin R, Kossov M, Kurashige H, Lamanna E, Lampén T, Lara V, Lefebure V, Lei F, Liendl M, Lockman W, Longo F, Magni S, Maire M, Medernach E, Minamimoto K, Mora de Freitas P, Morita Y, Murakami K, Nagamatu M, Nartallo R, Nieminen P, Nishimura T, Ohtsubo K, Okamura M, O'Neale S, Oohata Y, Paech K, Perl J, Pfeiffer A, Pia MG, Ranjard F, Rybin A, Sadilov S, Di Salvo E, Santin G, Sasaki T, Savvas N, Sawada Y, Scherer S, Sei S, Sirotenko V, Smith D, Starkov N, Stoecker H, Sulkimo J, Takahata M, Tanaka S, Tcherniaev E, Safai Tehrani E, Tropeano M, Truscott P, Uno H, Urban L, Urban P, Verderi M, Walkden A, Wander W, Weber H, Wellisch JP, Wenaus T, Williams DC, Wright D, Yamada T, Yoshida H, Zschiesche D (2003) Geant4—a simulation toolkit. Nucl Instrum Methods Phys Res Sect A 506(3):250–303. https://doi.org/10.1016/s0168-9002(03)01368-8
24. Pibida L, Hsieh E, Fuentes-Figueroa A, Hammond MM, Karam L (2006) Software studies for germanium detectors data analysis. Appl Radiat Isot 64(10–11):1313–1318. https://doi.org/10.1016/j.apradiso.2006.02.076
25. Taylor BN, Kuyatt CE (1994) Guidelines for Evaluating and Expressing the Uncertainty of NIST Measurement Results. NIST TN 1297
26. BIPM, IEC, IFCC, ILAC, ISO, IUPAC, IUPAP, OIML (2008) Evaluation of measurement data -Guide to the expression of uncertainty in measurement. JCGM